

Classification of symmetry properties of waveguide modes in presence of gain/losses, anisotropy/bianisotropy, or continuous/discrete rotational symmetry

ZHONGFEI XIONG¹, WEIJIN CHEN¹, PENG WANG¹, YUNTIAN CHEN^{1,2,*}

¹ School of Optical and Electronic Information, Huazhong University of Science and Technology, Wuhan, 430074, China

² Wuhan National Laboratory of Optoelectronics, Huazhong University of Science and Technology, Wuhan, China.

*yuntian@hust.edu.cn

Abstract: We study the symmetric properties of waveguide modes in presence of gain/losses, anisotropy/bianisotropy, or continuous/discrete rotational symmetry. We provide a comprehensive approach to identify the modal symmetry by constructing a 4×4 waveguide Hamiltonian and searching the symmetric operation in association with the corresponding waveguides. We classify the chiral/time reversal/parity/parity time/rotational symmetry for different waveguides, and provide the criterion for the aforementioned symmetry operations. Lastly, we provide examples to illustrate how the symmetry operations can be used to classify the modal properties from the symmetric relation between modal profiles of several different waveguides.

© 2017 Optical Society of America

OCIS codes: (230.7370) Waveguides;; (060.2310) Fiber optics; (060.2400) Fiber properties.

References and links

1. W. I. Fushchich, and A. G. Nikitin, *Symmetries of Maxwell's Equations* (D. Reidel Publishing Company, 1987).
2. K. Sakoda, *Optical Properties of Photonic crystals* (Springer-Verlag Berlin Heidelberg, 2005).
3. Dimitrios L. Sounas, and Andrea Alú, "Time-Reversal Symmetry Bounds on the Electromagnetic Response of Asymmetric Structures," *Phys. Rev. Lett.* **118**, 154302-154306 (2017).
4. M. Skorobogatiy, Steven A. Jacobs, Steven G. Johnson, and Yoel Fink, "Geometric variations in high index-contrast waveguides, coupled mode theory in curvilinear coordinates," *Opt. Express* **10**,(21), 1227-1243 (2002).
5. P. Chen, and Y. D. Chong, "Pseudo-Hermitian Hamiltonians generating waveguide mode evolution," *Phys. Rev. A*, **95**(6), 062113 (2017).
6. R. El-Ganainy, K. G. Makris, D. N. Christodoulides, and Z. H. Musslimani, "Theory of coupled optical PT-symmetric structures," *Opt. Lett.* **32**(17): 2632-2634(2007).
7. C. M. Bender, S. Boettcher, and P. N. Meisinger, "PT-symmetric quantum mechanics," *J. Math. Phys.* **40**: 2201 (1999).
8. B. A. Bernevig, and T. L. Hughes. *Topological insulators and topological superconductors* (Princeton University Press, 2013), Chap. 4.
9. L. Ge, A. D. Stone, "Parity-time symmetry breaking beyond one dimension: GePRX2014," *Physical Review X*, **4**(3), 031011 (2014).
10. J. Xu and Y. Chen, "General coupled mode theory in non-Hermitian waveguides," *Opt. Express* **23**(17), 22619-2627 (2015).
11. M. Hamermesh, *Group theory and its application to physical problems* (Courier Corporation, 1962) Chap. 3.
12. M. Srednicki, *Quantum field theory* (Cambridge University Press, 2007), Chap. 2,33.
13. COMSOL Multiphysics 5.2: a finite element analysis, solver and simulation software. URL <http://www.comsol.com/>
14. B. Richard, and L. Gagnon, *Optical Waveguide Modes: Polarization, Coupling and Symmetry* (McGraw-Hill, Inc., 2010), Chap. 3.
15. A. W. Snyder, and J. D. Love, *Optical waveguide theory* (Springer Science & Business Media, 2012).

1. Introduction

It is well-accepted that there are beautiful symmetric structures embedded in Maxwell's equations, i.e., the dual symmetry between electric and magnetic fields, time reversal symmetry, and many others as explained in [1]. Those symmetries on one hand could be used to simplify our understanding of mode hybridization associated with complicated optical structures [2], on the other hand impose certain constraints to electromagnetic response [3]. One also notes that certain optical structures based on combined symmetries of parity and time reversal \mathcal{PT} possess interesting features, i.e., real eigenvalues though the Hamiltonian being non-Hermitian, and exceptional points (EPs) where the transition of \mathcal{PT} symmetry breaking occurs. It is necessary to study and understand the general scenarios where those symmetries can be broken, leading to astonishing behaviors of light such as non-reciprocal or one-way propagation. In waveguides, there is an additional symmetry, i.e., translation symmetry along the propagation direction. Such translation symmetry ensures the modal wave number a constant value, i.e., propagation constant β , which is a typical terminology in waveguides. In analogy of a waveguide mode $\mathbf{E}(\mathbf{r}) = \mathbf{e}(x, y)e^{-i\beta z}$ to a wave-function $\Psi(\mathbf{r}, t) = \Psi(\mathbf{r})e^{-iEt}$ associated with the stationary Schrödinger equation $H\Psi(\mathbf{r}) = E\Psi(\mathbf{r})$, z plays the role of time t , and β plays the role of energy E [4, 5].

In isotropic waveguide, the negative propagating modes ($-\beta$) can be considered as a perfect image of the forward propagating modes (β). It is interesting to ask how the forward and backward propagating modes are related, if the waveguide materials contain gain/losses, anisotropy, or bianisotropy? One also notes that if the waveguide cross-section contains rotational symmetries, the polarization modes associated with the same field configuration may or may not degenerate. Though those results are well documented in the literatures, there is no systematic approach to classify the symmetry properties of waveguide mode using the equivalent Hamiltonian, considering the analogy of the wave equation of the waveguides with the stationary Schrödinger equation. Along this line, it is important to point out the waveguide mode are vector fields, in contrast to the scalar wave function in Schrödinger equation.

In this work, we derive the exact Hamiltonian of the waveguide from Maxwell's equations. In our formulation, we take into account the vectorial nature of electromagnetic fields in the equivalent waveguide Hamiltonian, which resembles Dirac equation accounting for electrons with positive/negative energies and up/down spin states. By construction, we search for the symmetry operations associated with the Hamiltonian to classify the symmetry properties of waveguide modes in presence of gain/losses, anisotropy/bianisotropy, or continuous/discrete rotational symmetry in the geometric cross-section of the waveguides.

The paper is organized as follows: In Section 2, we outline the construction of Hamiltonian for the waveguide as well as the description of the symmetry operations. In Section 3, we apply the symmetry operations to the Hamiltonian of different waveguides, and to classify the symmetric properties of the waveguide modes. Finally, Section 4 concludes the paper.

2. Theory

2.1. Waveguide Hamiltonian

We take a time harmonic dependence $e^{i\omega t}$ for the electromagnetic waves throughout this paper. The source-free Maxwell's equations for general bianisotropic waveguide read as follows,

$$\begin{aligned} [\nabla \times + Ik_0\tilde{\chi}_{he}] \mathbf{e}_{3d}(x, y, z) + Ik_0(\tilde{\boldsymbol{\mu}}_r)\mathbf{h}_{3d}(x, y, z) &= 0, \\ [\nabla \times - Ik_0\tilde{\chi}_{eh}] \mathbf{h}_{3d}(x, y, z) - Ik_0(\tilde{\boldsymbol{\epsilon}}_r)\mathbf{e}_{3d}(x, y, z) &= 0, \end{aligned} \quad (1)$$

where $e_{3d}(x, y, z) = e_{2d}(x, y)e^{-i\beta z} = e_{2d}^t(x, y)e^{-i\beta z} + e_{2d}^z(x, y)e^{-i\beta z}$, $h_{3d}(x, y, z) = h_{2d}(x, y)e^{-i\beta z} = h_{2d}^t(x, y)e^{-i\beta z} + e_{2d}^z(x, y)e^{-i\beta z}$, $\bar{\epsilon}_r = \begin{pmatrix} \bar{\epsilon}_r^{tt} & \bar{\epsilon}_r^{tz} \\ \bar{\epsilon}_r^{zt} & \bar{\epsilon}_r^{zz} \end{pmatrix} = \begin{pmatrix} \epsilon_r^{xx} & \epsilon_r^{xy} & \epsilon_r^{xz} \\ \epsilon_r^{yx} & \epsilon_r^{yy} & \epsilon_r^{yz} \\ \epsilon_r^{zx} & \epsilon_r^{zy} & \epsilon_r^{zz} \end{pmatrix}$, $\bar{\mu}_r = \begin{pmatrix} \bar{\mu}_r^{tt} & \bar{\mu}_r^{tz} \\ \bar{\mu}_r^{zt} & \bar{\mu}_r^{zz} \end{pmatrix} = \begin{pmatrix} \mu_r^{xx} & \mu_r^{xy} & \mu_r^{xz} \\ \mu_r^{yx} & \mu_r^{yy} & \mu_r^{yz} \\ \mu_r^{zx} & \mu_r^{zy} & \mu_r^{zz} \end{pmatrix}$, and $\bar{\chi}_{he} = -\bar{\chi}_{eh}^T = i\bar{\chi} = i \begin{pmatrix} \chi_{xx} & \chi_{xy} \\ \chi_{yx} & \chi_{yy} \end{pmatrix}$. Equation (1) can be reformulated into 4 components equation, by eliminating the $e_{2d}^z(x, y)$ and $h_{2d}^z(x, y)$ via the expressions $e_{2d}^z(x, y) = \frac{\nabla_t \times h_{2d}^t(x, y) - Ik_0 \bar{\epsilon}_r^{zt} \cdot e_{2d}^t(x, y)}{Ik_0 \bar{\epsilon}_r^{zz}}$ and $h_{2d}^z(x, y) = -\frac{\nabla_t \times e_{2d}^t(x, y) + Ik_0 \bar{\mu}_r^{zt} \cdot h_{2d}^t(x, y)}{Ik_0 \bar{\mu}_r^{zz}}$. The resulted equations for the in-plane field components can be written in a compact form,

$$H\Psi = \beta\Psi, \quad (2)$$

where the Hamiltonian H given by

$$H = \begin{pmatrix} -i\partial_x \frac{\bar{\epsilon}_r^{zx}}{\bar{\epsilon}_r^{zz}} - i\frac{\mu_r^{yz}}{\mu_r^{zz}} \partial_y + ik_0 \chi_{yx} & -i\partial_x \frac{\bar{\epsilon}_r^{zy}}{\bar{\epsilon}_r^{zz}} + i\frac{\mu_r^{yz}}{\mu_r^{zz}} \partial_x + ik_0 \chi_{yy} & -\partial_x \frac{\partial_y}{k_0 \bar{\epsilon}_r^{zz}} - \frac{k_0}{\mu_r^{zz}} \mu_r^{yz} \mu_r^{zx} + k_0 \bar{\mu}_r^{yx} & \partial_x \frac{\partial_y}{k_0 \bar{\epsilon}_r^{zz}} - \frac{k_0}{\mu_r^{zz}} \mu_r^{yz} \mu_r^{zy} + k_0 \bar{\mu}_r^{yy} \\ -i\partial_y \frac{\bar{\epsilon}_r^{zx}}{\bar{\epsilon}_r^{zz}} + i\frac{\mu_r^{yz}}{\mu_r^{zz}} \partial_y - ik_0 \chi_{xx} & -i\partial_y \frac{\bar{\epsilon}_r^{zy}}{\bar{\epsilon}_r^{zz}} - i\frac{\mu_r^{yz}}{\mu_r^{zz}} \partial_x - ik_0 \chi_{xy} & -\partial_y \frac{\partial_x}{k_0 \bar{\epsilon}_r^{zz}} + \frac{k_0}{\mu_r^{zz}} \mu_r^{xz} \mu_r^{zx} - k_0 \bar{\mu}_r^{xx} & \partial_y \frac{\partial_x}{k_0 \bar{\epsilon}_r^{zz}} + \frac{k_0}{\mu_r^{zz}} \mu_r^{xz} \mu_r^{zy} - k_0 \bar{\mu}_r^{xy} \\ \partial_x \frac{\partial_y}{k_0 \bar{\mu}_r^{zz}} + \frac{k_0}{\bar{\epsilon}_r^{zz}} \bar{\epsilon}_r^{yz} \bar{\epsilon}_r^{zx} - k_0 \bar{\epsilon}_r^{yx} & -\partial_x \frac{\partial_y}{k_0 \bar{\mu}_r^{zz}} + \frac{k_0}{\bar{\epsilon}_r^{zz}} \bar{\epsilon}_r^{yz} \bar{\epsilon}_r^{zy} - k_0 \bar{\epsilon}_r^{yy} & -i\partial_x \frac{\mu_r^{zx}}{\mu_r^{zz}} - i\frac{\bar{\epsilon}_r^{yz}}{\bar{\epsilon}_r^{zz}} \partial_y + ik_0 \chi_{xy} & -i\partial_x \frac{\mu_r^{zy}}{\mu_r^{zz}} + i\frac{\bar{\epsilon}_r^{yz}}{\bar{\epsilon}_r^{zz}} \partial_x + ik_0 \chi_{yy} \\ \partial_y \frac{\partial_x}{k_0 \bar{\mu}_r^{zz}} - \frac{k_0}{\bar{\epsilon}_r^{zz}} \bar{\epsilon}_r^{xz} \bar{\epsilon}_r^{zx} + k_0 \bar{\epsilon}_r^{xx} & -\partial_y \frac{\partial_x}{k_0 \bar{\mu}_r^{zz}} - \frac{k_0}{\bar{\epsilon}_r^{zz}} \bar{\epsilon}_r^{xz} \bar{\epsilon}_r^{zy} + k_0 \bar{\epsilon}_r^{xy} & -i\partial_y \frac{\mu_r^{zx}}{\mu_r^{zz}} + i\frac{\bar{\epsilon}_r^{xz}}{\bar{\epsilon}_r^{zz}} \partial_y - ik_0 \chi_{xx} & -i\partial_y \frac{\mu_r^{zy}}{\mu_r^{zz}} - i\frac{\bar{\epsilon}_r^{xz}}{\bar{\epsilon}_r^{zz}} \partial_x - ik_0 \chi_{yx} \end{pmatrix}$$

and $\Psi = [e_x(x, y), e_y(x, y), h_x(x, y), h_y(x, y)]^T$ is the eigenstate, which contains the in-plane field components. In Eq. (2), we limit our self to study the mode properties of the waveguide within the truncated mode set, with particular emphasis on the symmetry relations among the polarizations, as well as that between the forward propagating modes and the backward propagating modes. The truncated mode set is defined as the waveguide modes, which share the field configuration labeled by the same quantum numbers in the traverse plane. For simplicity, we investigate the waveguides with single core structure, the medium of which could be active, lossy, anisotropic or bianisotropic. The geometric cross section of the waveguide core structure could be irregular, or highly symmetric. The background is homogeneous and isotropic.

Corresponding to the 4×4 matrix form Hamiltonian, there will be 4 eigenmodes Ψ_1^+ , Ψ_2^+ , Ψ_1^- and Ψ_2^- in the truncated mode set, with eigenvalue being β_1^+ , β_2^+ , β_1^- and β_2^- respectively. The superscript $+$ ($-$) indicates forward (backward) propagating modes, and we note a pair of orthogonal polarization modes in same direction with subscript 1 or 2. Once the waveguide Hamiltonian is known, the degeneracy of the modes within the truncated mode set can be classified by searching proper symmetry operations.

In the paper, we concern waveguiding mainly by the refractive index contrast. Thus, the waveguide can be sliced into regions with piece-wise constant material properties. To perform modal analysis of waveguide, one finds the eigenfields of each region, and then apply the boundary condition to connect the fields from different regions such that the eigenfields of the waveguide can be obtained. This procedure shows that the final eigenfield of the waveguide can be seen as certain combination of the eigenfield of each individual region, though the boundary condition determines how the eigenfields from different region are combined. In any case, the final eigenfield of the waveguide mode obeys the same symmetry as the eigenfield of each individual region, provided the same modal wave number β is selected. Thus, the study on the symmetry properties of the waveguide mode can be reduced to analysis the symmetry properties of the eigenfield of each individual region, with no need to concern the boundary conditions. In our settings, the background of the waveguide core is air, the symmetry relation of the waveguide mode is essentially determined by the waveguide core, which is our focus in the following sections.

2.2. Chiral symmetry

We study the degeneracy between opposite propagating modes (Ψ_1^+ and Ψ_1^- or Ψ_2^+ and Ψ_2^-). Here, an unitary matrix

$$\sigma = \begin{pmatrix} 1 & 0 & 0 & 0 \\ 0 & 1 & 0 & 0 \\ 0 & 0 & -1 & 0 \\ 0 & 0 & 0 & -1 \end{pmatrix}, \quad (3)$$

is introduced as an operator to describe a chiral transformation. As the operator σ acts on a state Ψ , it reverses the sign of transverse magnetic field while the transverse electric fields remain unchanged, and the original and transformed transverse electromagnetic fields can be seen as left-handed and right-handed systems. Since the Poynting vector \mathbf{P} is defined as $\mathbf{P} = \mathbf{E} \times \mathbf{H}$, the chiral operation σ changes the propagation direction of power flow, thereby builds the connection between forward and backward propagating modes. If the terms $\bar{\epsilon}_r^{zt}$, $\bar{\epsilon}_r^{tz}$, $\bar{\mu}_r^{zt}$, $\bar{\mu}_r^{tz}$ and $\bar{\chi}$ in Hamiltonian H vanish, then H in Eq. (2) is reduced to,

$$H = \begin{pmatrix} 0 & 0 & -\partial_x \frac{\partial_y}{k_0 \bar{\epsilon}_r^{zz}} + k_0 \bar{\mu}_r^{yx} & \partial_x \frac{\partial_x}{k_0 \bar{\epsilon}_r^{zz}} + k_0 \bar{\mu}_r^{yy} \\ 0 & 0 & -\partial_y \frac{\partial_y}{k_0 \bar{\epsilon}_r^{zz}} - k_0 \bar{\mu}_r^{xx} & \partial_y \frac{\partial_x}{k_0 \bar{\epsilon}_r^{zz}} - k_0 \bar{\mu}_r^{xy} \\ \partial_x \frac{\partial_y}{k_0 \bar{\mu}_r^{zz}} - k_0 \bar{\epsilon}_r^{yx} & -\partial_x \frac{\partial_x}{k_0 \bar{\mu}_r^{zz}} - k_0 \bar{\epsilon}_r^{yy} & 0 & 0 \\ \partial_y \frac{\partial_y}{k_0 \bar{\mu}_r^{zz}} + k_0 \bar{\epsilon}_r^{xx} & -\partial_y \frac{\partial_x}{k_0 \bar{\mu}_r^{zz}} + k_0 \bar{\epsilon}_r^{xy} & 0 & 0 \end{pmatrix}. \quad (4)$$

A close examination shows that the following relation for the reduced waveguide Hamiltonian H in Eq. (4) holds,

$$\sigma H \sigma^{-1} = -H, \quad (5)$$

which means if β_1 is the eigenvalue of H with eigenstate Ψ_1 , the $-\beta_1$ would also be the eigenvalue with eigenstate $\sigma\Psi_1$. In other words, for a given forward propagating mode, there is a degenerate backward propagating mode, and the eigen-fields transform to each other by the symmetry operation σ , provided that the constraints on $\bar{\epsilon}_r$, $\bar{\mu}_r$ and $\bar{\chi}$ are fulfilled.

2.3. Time reversal symmetry

Next, we introduce the time reversal operator $\mathcal{T} : \hat{p} \rightarrow -\hat{p}, i \Rightarrow -i$, where \hat{p} is the momentum operator [6, 7]. In general, this operator can be represented as $\mathcal{T} = UK$, where U is a unitary matrix and K is complex conjugation [8]. The operator σ used in chiral symmetry operation is an unitary matrix, and will be used here to replace U , leading to the time reversal operator as follows,

$$\mathcal{T} = \sigma K. \quad (6)$$

As the operator K acts on the Hamiltonian, all the i in Eq. (2) reverses sign, and all the elements in the permittivity tensor $\bar{\epsilon}_r$, permeability tensor $\bar{\mu}_r$ and $\bar{\chi}$ in Eq. (2) take the complex conjugate. If the waveguide is invariant under time reversal operation, which requires all the these elements in material tensors, i.e., $\bar{\epsilon}_r$, $\bar{\mu}_r$ and $\bar{\chi}$ to be real numbers, we shall have,

$$\mathcal{T} H \mathcal{T}^{-1} = -H \quad (7)$$

Similar to Eq. (4), the Hamiltonian also reverses sign under the time reversal operation. Therefore, as a result of Eq. (7), the forward and backward propagating modes are degenerated, but up to a sign difference in the eigenvalues (β), the eigenstates are related by operator \mathcal{T} . In contrast to chiral symmetry operator, we don't necessarily need the reduced Hamiltonian in Eq. (4) for \mathcal{T} operator, but the time reversal symmetry indeed requires that all the elements in the material tensors ($\bar{\epsilon}_r$, $\bar{\mu}_r$ and $\bar{\chi}$) to be real. And the transformation between the fields of the degenerate

modes, not only needs σ , but also needs take the complex conjugate. Despite those differences in chiral symmetry operator and the time reversal operator, both can be applied to scenarios, in which $\bar{\chi}$ is zero, $\bar{\epsilon}_r$, $\bar{\mu}_r$ are real and without tz, zt elements, and the two symmetry operation yields exactly the same results. Same as chiral symmetry, time reversal operator \mathcal{T} doesn't perform any action on space, thus there is no constraint on the geometry structure of waveguide.

2.4. Parity symmetry

We proceed to discuss the symmetry operation that changes the coordinates, for example, parity operator \mathcal{P} , $\mathbf{r} \rightarrow -\mathbf{r}$, $\hat{p} \rightarrow -\hat{p}$, where \mathbf{r} is the position operator and only contains transverse coordinate (x, y) [6, 7]. The optical properties of waveguide are essentially determined by the spatial dependent permittivity and permeability, i.e., $\bar{\epsilon}_r(\mathbf{r})$ and $\bar{\mu}_r(\mathbf{r})$. Considering $\bar{\chi}=0$, Eq. (2) can be reformulated as:

$$H(\mathbf{r}, \bar{\epsilon}_r(\mathbf{r}), \bar{\mu}_r(\mathbf{r})) \Psi(\mathbf{r}) = \beta \Psi(\mathbf{r}), \quad (8)$$

the first \mathbf{r} in Hamiltonian H represents the coordinates that get differentiated, all the rest \mathbf{r} in Eq. (8) simply represents the spatial dependence of material tensors and wave-function. The parity operator \mathcal{P} also contains a unitary matrix σ and an operator that reverses coordinate. As the operator \mathcal{P} acts on Hamiltonian in Eq. (8), one shall have the following equation

$$\mathcal{P}H(\mathbf{r}, \bar{\epsilon}_r(\mathbf{r}), \bar{\mu}_r(\mathbf{r})) \mathcal{P}^{-1} = \sigma H(-\mathbf{r}, \bar{\epsilon}_r(-\mathbf{r}), \bar{\mu}_r(-\mathbf{r})) \sigma^{-1} = -H(\mathbf{r}, \bar{\epsilon}_r(-\mathbf{r}), \bar{\mu}_r(-\mathbf{r})). \quad (9)$$

If the cross-section of the waveguide is invariant under \mathcal{P} , i.e., $\bar{\epsilon}_r(-\mathbf{r}) = \bar{\epsilon}_r(\mathbf{r})$ and $\bar{\mu}_r(-\mathbf{r}) = \bar{\mu}_r(\mathbf{r})$, one obtains

$$\begin{aligned} \mathcal{P}H(\mathbf{r}, \bar{\epsilon}_r(\mathbf{r}), \bar{\mu}_r(\mathbf{r})) \mathcal{P}^{-1} \mathcal{P} \Psi(\mathbf{r}) &= -H(\mathbf{r}, \bar{\epsilon}_r(\mathbf{r}), \bar{\mu}_r(\mathbf{r})) \mathcal{P} \Psi(\mathbf{r}) = \beta \sigma \Psi(-\mathbf{r}), \\ H(\mathbf{r}, \bar{\epsilon}_r(\mathbf{r}), \bar{\mu}_r(\mathbf{r})) \sigma \Psi(-\mathbf{r}) &= -\beta \sigma \Psi(-\mathbf{r}). \end{aligned} \quad (10)$$

Consequently, $\mathcal{P} \Psi(\mathbf{r}) = \sigma \Psi(-\mathbf{r})$ is the degenerated mode (opposite propagation direction) of original state $\Psi(\mathbf{r})$. In comparison with Eq. (5) in chiral symmetry, parity symmetry operation does not require that those components ($\bar{\epsilon}_r^{zt}$, $\bar{\epsilon}_r^{tz}$, $\bar{\mu}_r^{zt}$ and $\bar{\mu}_r^{tz}$) vanish, but reverses the coordinates of the fields before performing σ -operation. Intuitively, it can be understood that the presence of $\bar{\epsilon}_r^{tz}$ or $\bar{\epsilon}_r^{zt}$ elements in $\bar{\epsilon}_r$ or $\bar{\mu}_r$ breaks the chiral symmetry between the forward and backward propagating modes, while the presence of parity symmetry in the structure of cross-section restore it. When $\bar{\chi}$ can't be ignored, the conclusion will also be kept under $\bar{\chi}(\mathbf{r}) = -\bar{\chi}(-\mathbf{r})$.

2.5. \mathcal{PT} symmetry

In the time reversal/parity symmetry operation, we have proved there is a definite relation between the forward and backward propagating modes that is guaranteed by \mathcal{P}/\mathcal{T} symmetry. In this subsection, we continue to discuss the symmetric properties induced by combining the two symmetry operations together, i.e., \mathcal{PT} symmetry, which has been examined extensively in the last few years [5–7, 9, 10]. As the operator \mathcal{P} and \mathcal{T} both act on Hamiltonian H , one obtains $\mathcal{PT}H(\hat{p}, \mathbf{r}, t) (\mathcal{PT})^{-1} = H^*(\hat{p}, -\mathbf{r}, -t)$. If the optical systems are \mathcal{PT} symmetric (here we only concerns isotropic medium), i.e., $\epsilon_r(\mathbf{r}) = \epsilon_r^*(-\mathbf{r})$, $\mu_r(\mathbf{r}) = \mu_r^*(-\mathbf{r})$, one find the waveguide Hamiltonian H commutes with the \mathcal{PT} operator, i.e., $\mathcal{PT}H(\mathcal{PT})^{-1} = H$, leading to

$$\mathcal{PT}H(\mathbf{r}, \bar{\epsilon}_r(\mathbf{r}), \bar{\mu}_r(\mathbf{r})) (\mathcal{PT})^{-1} \mathcal{PT} \Psi(\mathbf{r}) = H(\mathbf{r}, \bar{\epsilon}_r(\mathbf{r}), \bar{\mu}_r(\mathbf{r})) \Psi^*(-\mathbf{r}) = \beta^* \Psi^*(-\mathbf{r}). \quad (11)$$

From Eq. (8) and Eq. (11), one immediately finds out the fact that if $\Psi(\mathbf{r})$ is the eigenmode for Hamiltonian with eigenvalue β , its complex conjugate partner with reversed coordinates $\Psi^*(-\mathbf{r})$ would also be the eigenmode with eigenvalue β^* . Before the \mathcal{PT} symmetry is broken, the eigenvalues are always real number, with $\beta^* = \beta$ and $\Psi^*(-\mathbf{r}) = \Psi(\mathbf{r})$. Once the \mathcal{PT} symmetry is broken, β^* and β are different values, $\Psi^*(-\mathbf{r})$ and $\Psi(\mathbf{r})$ are separated eigenstates of H . The media can be anisotropy in time reversal symmetry or parity symmetry respectively, actually, the media under \mathcal{PT} symmetry can also be anisotropy (See Table. (1)).

2.6. Rotation symmetry

We continue to study the degeneracy between the polarization states Ψ_1, Ψ_2 due to the rotational symmetry of the cross-section of waveguides. Considering the structure symmetry of the cross-section can be encoded into the optical properties of the material, we use Eq. (8) that explicitly encloses the coordinate-dependent material tensors, i.e., $\bar{\epsilon}_r(\mathbf{r})$ and $\bar{\mu}_r(\mathbf{r})$. Due to the symmetry requirement, we only consider isotropic waveguides such as ordinary optical fiber for simplicity. To this end, the Hamiltonian H can be reduced as,

$$H(\mathbf{r}, \bar{\epsilon}_r(\mathbf{r}), \bar{\mu}_r(\mathbf{r})) = \begin{pmatrix} 0 & 0 & -\partial_x \frac{\partial_y}{k_0 \epsilon_r} & \partial_x \frac{\partial_x}{k_0 \epsilon_r} + k_0 \mu_r \\ 0 & 0 & -\partial_y \frac{\partial_y}{k_0 \epsilon_r} - k_0 \mu_r & \partial_y \frac{\partial_x}{k_0 \epsilon_r} \\ \partial_x \frac{\partial_y}{k_0 \mu_r} & -\partial_x \frac{\partial_x}{k_0 \mu_r} - k_0 \epsilon_r & 0 & 0 \\ \partial_y \frac{\partial_y}{k_0 \mu_r} + k_0 \epsilon_r & -\partial_y \frac{\partial_x}{k_0 \mu_r} & 0 & 0 \end{pmatrix}. \quad (12)$$

If an eigenstates $\Psi_1(\mathbf{r})$ in Eq. (8) can be rotated anticlockwise by a constant angle θ to another eigenstates $\Psi_2(\mathbf{r})$, which can be described by the following equation,

$$\Psi_2(\mathbf{r}) = P(\theta) \Psi_1(R^{-1}(\theta)\mathbf{r}), \quad (13)$$

where the polarization rotation operator $P_R(\theta) = \begin{pmatrix} \cos \theta & -\sin \theta & 0 & 0 \\ \sin \theta & \cos \theta & 0 & 0 \\ 0 & 0 & \cos \theta & -\sin \theta \\ 0 & 0 & \sin \theta & \cos \theta \end{pmatrix}$, and the

coordinate rotation operator $R(\theta) = \begin{pmatrix} \cos \theta & -\sin \theta \\ \sin \theta & \cos \theta \end{pmatrix}$. As can be seen, the rotation of the vector field is in sharp contrast to the rotation of a scalar field: if one wants to rotate a scalar anticlockwise, one just rotates the coordinate system clockwise by same angle; as for vector field, one need to consider the rotation between the field components beside the rotation of each components, as described by Eq. (13). As a side remark, Ψ_1 and Ψ_2 can be considered as the polarization modes associated with the same field configuration, such that the in-plane vector fields of the two modes are always perpendicular, i.e., $\Psi_2 = P_R(\frac{\pi}{2}) \Psi_1$.

As the operator $P_R(\theta)$ acts on the Hamiltonian H , see Eq. (12), one shall obtain,

$$P_R(\theta) H(\mathbf{r}, \bar{\epsilon}_r(\mathbf{r}), \bar{\mu}_r(\mathbf{r})) P_R^{-1}(\theta) = H(R(\theta)\mathbf{r}, \bar{\epsilon}_r(\mathbf{r}), \bar{\mu}_r(\mathbf{r})) \\ = \begin{pmatrix} 0 & 0 & -\partial_u \frac{\partial_v}{k_0 \epsilon_r} & \partial_u \frac{\partial_u}{k_0 \epsilon_r} + k_0 \mu_r \\ 0 & 0 & -\partial_v \frac{\partial_v}{k_0 \epsilon_r} - k_0 \mu_r & \partial_v \frac{\partial_u}{k_0 \epsilon_r} \\ \partial_u \frac{\partial_v}{k_0 \mu_r} & -\partial_u \frac{\partial_u}{k_0 \mu_r} - k_0 \epsilon_r & 0 & 0 \\ \partial_v \frac{\partial_v}{k_0 \mu_r} + k_0 \epsilon_r & -\partial_v \frac{\partial_u}{k_0 \mu_r} & 0 & 0 \end{pmatrix} \quad (14)$$

where $\begin{pmatrix} u \\ v \end{pmatrix} = \begin{pmatrix} \cos \theta & -\sin \theta \\ \sin \theta & \cos \theta \end{pmatrix} \begin{pmatrix} x \\ y \end{pmatrix} = R(\theta)\mathbf{r}$. It's interesting to note the fact that the operator $P_R(\theta)$ acting on H is equivalent to rotate the differential Coordinates in H , with $\bar{\epsilon}_r(\mathbf{r})$ and $\bar{\mu}_r(\mathbf{r})$ unchanged. With the substitution of Eq. (13) and Eq. (14) into Eq. (8), one obtains

$$P_R H(R^{-1}\mathbf{r}, \bar{\epsilon}_r(R^{-1}\mathbf{r}), \bar{\mu}_r(R^{-1}\mathbf{r})) P_R^{-1} \Psi_1(R^{-1}\mathbf{r}) = \beta_1 P_R \Psi_1(R^{-1}\mathbf{r}), \\ H(\mathbf{r}, \bar{\epsilon}_r(R^{-1}\mathbf{r}), \bar{\mu}_r(R^{-1}\mathbf{r})) \Psi_2(\mathbf{r}) = \beta_1 \Psi_2(\mathbf{r}). \quad (15)$$

If the cross-section of waveguide is invariant under the rotation of θ , we can get $H(\mathbf{r}, \bar{\epsilon}_r(\mathbf{r}), \bar{\mu}_r(\mathbf{r})) \Psi_2(\mathbf{r}) = \beta_1 \Psi_2(\mathbf{r})$ from Eq. (15), thus establishes the symmetric (degenerate)

relation between the two polarization modes. When the media is on longer isotropy, we can get the same conclusion with constraint that $\hat{R}\bar{\epsilon}_r(R^{-1}\mathbf{r})\hat{R}^{-1} = \bar{\epsilon}_r(\mathbf{r})$, $\hat{R}\bar{\mu}_r(R^{-1}\mathbf{r})\hat{R}^{-1} = \bar{\mu}_r(\mathbf{r})$ and

$$R\bar{\chi}(R^{-1}\mathbf{r})R^{-1} = \bar{\chi}(\mathbf{r}), \text{ where } \hat{R} = \begin{pmatrix} \cos \theta & -\sin \theta & 0 \\ \sin \theta & \cos \theta & 0 \\ 0 & 0 & 1 \end{pmatrix}.$$

Table 1. Symmetry properties of waveguide modes in the truncated mode set

	Symmetry	Degeneracy	Constraints
Chiral symmetry	$\sigma H \sigma^{-1} = -H$	$\beta^- = -\beta^+$ $\Psi^- = \sigma \Psi^+$	$\bar{\epsilon}_r^{zt} = \bar{\epsilon}_r^{tz} = 0$ $\bar{\mu}_r^{zt} = \bar{\mu}_r^{tz} = 0$ and no $\bar{\chi}$
Time reversal symmetry	$\mathcal{T} H \mathcal{T}^{-1} = -H$	$\beta^- = -(\beta^+)^*$ $\Psi^- = \mathcal{T} \Psi^+ = \sigma (\Psi^+)^*$	$\bar{\epsilon}_r, \bar{\mu}_r$ and $\bar{\chi}$ are real
Parity symmetry	$\mathcal{P} H \mathcal{P}^{-1} = -H$	$\beta^- = -\beta^+$ $\Psi^-(\mathbf{r}) = \mathcal{P} \Psi^+(\mathbf{r}) = \sigma \Psi^+(-\mathbf{r})$	$\bar{\epsilon}_r(\mathbf{r}) = \bar{\epsilon}_r(-\mathbf{r})$ $\bar{\mu}_r(\mathbf{r}) = \bar{\mu}_r(-\mathbf{r})$ $\bar{\chi}(\mathbf{r}) = -\bar{\chi}(-\mathbf{r})$
PT symmetry	$\mathcal{P} \mathcal{T} H (\mathcal{P} \mathcal{T})^{-1} = H$	$\Psi_{\beta^*}(\mathbf{r}) = \mathcal{P} \mathcal{T} \Psi_{\beta}(\mathbf{r}) = \Psi_{\beta}^*(-\mathbf{r})$	$\bar{\epsilon}_r(\mathbf{r}) = \bar{\epsilon}_r^*(-\mathbf{r})$ $\bar{\mu}_r(\mathbf{r}) = \bar{\mu}_r^*(-\mathbf{r})$ $\bar{\chi}(\mathbf{r}) = -\bar{\chi}^*(-\mathbf{r})$
Rotation symmetry	$P_R H (R^{-1}\mathbf{r}) P_R^{-1} = H(\mathbf{r})$	$\beta_2 = \beta_1$ $\Psi_2(\mathbf{r}) = P_R \Psi_1(R^{-1}\mathbf{r})$	$\hat{R}\bar{\epsilon}_r(R^{-1}\mathbf{r})\hat{R}^{-1} = \bar{\epsilon}_r(\mathbf{r})$ $\hat{R}\bar{\mu}_r(R^{-1}\mathbf{r})\hat{R}^{-1} = \bar{\mu}_r(\mathbf{r})$ $R\bar{\chi}(R^{-1}\mathbf{r})R^{-1} = \bar{\chi}(\mathbf{r})$

2.7. Transformation of vector field

To get a comprehensive impression of symmetry operations discussed in this paper, we list the five different symmetry operations in Table. (1). The first three symmetry operations are used to establish the symmetric relation between the forward and backward propagating modes, and the last two symmetry operations establish the relationship between two modes with same propagating direction.

The transverse electromagnetic field components, which are the eigenfunction Ψ of waveguide Hamiltonian, is essentially a vector field. Considering the sharp contrast between rotating vector fields and rotating scalar fields, it is necessary to give formal expressions to describe how the vector and scalar fields are rotated. According to [11, 12], as a rotating operator O_R acts on a scalar field (for example, x component of electric field e_x) and a vector field (for example, transverse electric field $\mathbf{e}_t = (e_x, e_y)^T$), one shall have,

$$O_R e_x(\mathbf{r}) = e_x(R^{-1}\mathbf{r}), \quad (16)$$

and

$$O_R \mathbf{e}_t(\mathbf{r}) = \mathcal{R} \mathbf{e}_t(R^{-1}\mathbf{r}), \quad (17)$$

where the operator R is the aforementioned coordinate rotating operator, and \mathcal{R} the rotating operation that reshuffles different components of the vector fields. Rotating a scalar field is equivalent to rotating coordinates as described in Eq. (16). Evident from (17), there are more evolved in the rotation of a vector field. In short, we could decompose the rotation of vector field into two steps: (1) reshuffling the components of the vector field, and (2) coordinate rotation. Thus, the action of step (1) $\mathcal{R} \mathbf{e}_t(\mathbf{r})$ and step (2) $\mathbf{e}_t(R^{-1}\mathbf{r})$ are very different, one acting on the field components, the other on the coordinates of each components of the vector field.

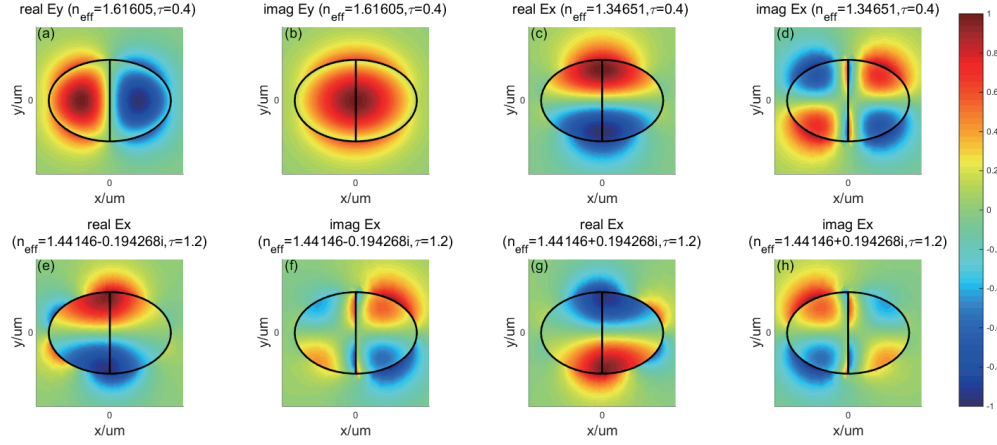


Fig. 1. The x and y-components of the electric field for a pair of modes supported by the gain-loss balanced waveguides before and after the exceptional point. The fields before/after EP are shown in the first/second row. (a/b) The dominating electric field component, i.e., $\text{Re}(E_y)/\text{Im}(E_y)$, for the mode with $n_{\text{eff}} = 1.61605$; (c/d) the dominating electric field component, i.e., $\text{Re}(E_x)/\text{Im}(E_x)$, for the mode with $n_{\text{eff}} = 1.34651$. If the \mathcal{P} operation is applied, i.e., $\mathbf{r} \rightarrow -\mathbf{r}$, the real parts of the fields in (a,c) remains unchanged, while the imaginary parts of the fields in (b,d) change sign. The x-components of the electric field, including $\text{Re}(E_x)$ and $\text{Im}(E_x)$, for the two mode with conjugate $n_{\text{eff}} = 1.44146 \pm 0.194268i$ are shown (e-h). Evidently, the field plot in (e) can be transformed to that in (g) under \mathcal{P} operation. Similarly, the field plot in (f) can be transformed to that in (h) under \mathcal{P} operation, but up to a sign difference.

We further explain the subtle difference via rotating the electric field, i.e., represented by the position-dependent arrows. The \mathcal{R} operator in (17) acts on the electric field directly (same as σ , \mathcal{T} and P_R in Table. (1)), only changes the orientation of the arrow without moving the position of arrows, while the R operation in $\mathbf{e}_t (R^{-1}\mathbf{r})$ acts on the coordinates of the arrows, only changes the arrow position without changing the orientation of the arrow.

In Section 2.2 and 2.3, we only reshuffle the components of the vector field without touching on the coordinates. Thus, the operator σ in chiral symmetry and the operator \mathcal{T} in time reversal symmetry essentially belongs to step (1). In Sections 2.4, 2.5 and 2.6, those symmetry operations can be considered as combined operations of step (1) and step(2).

3. Results and discussions

3.1. \mathcal{PT} symmetry in gain-loss balanced waveguides

The most commonly used optical structures in \mathcal{PT} symmetry systems are gain-loss balanced waveguides. Here, we consider a simple example, see Fig. 1, to illustrate the symmetric relations of the vector fields of a single mode or between two conjugated modes under the \mathcal{PT} symmetry operation, depending on whether the \mathcal{PT} symmetry breaking occurs or not. We consider elliptical waveguide core with the semi-major (semi-minor) of $1.5\mu\text{m}$ ($1\mu\text{m}$). The material in the waveguide core region is isotropic, i.e., $\epsilon_r = 4 - i\tau$ on the left hand side, while $\epsilon_r = 4 + i\tau$ on the right hand side. The waveguide core is embedded in air with operation wavelength $4\mu\text{m}$. The eigen-fields and eigenvalues β of the gain-loss balanced waveguides, as well as others throughout the paper are obtained by full-wave simulations using COMSOL MULTIPHYSICS [13]. As the magnitude of gain/losses (τ) increases, \mathcal{PT} symmetry breaking occurs, the real parts of two eigenvalues β merger together and the overlapped imaginary part of the two eigenvalues, i.e., $\text{Im}(\beta) = 0$,

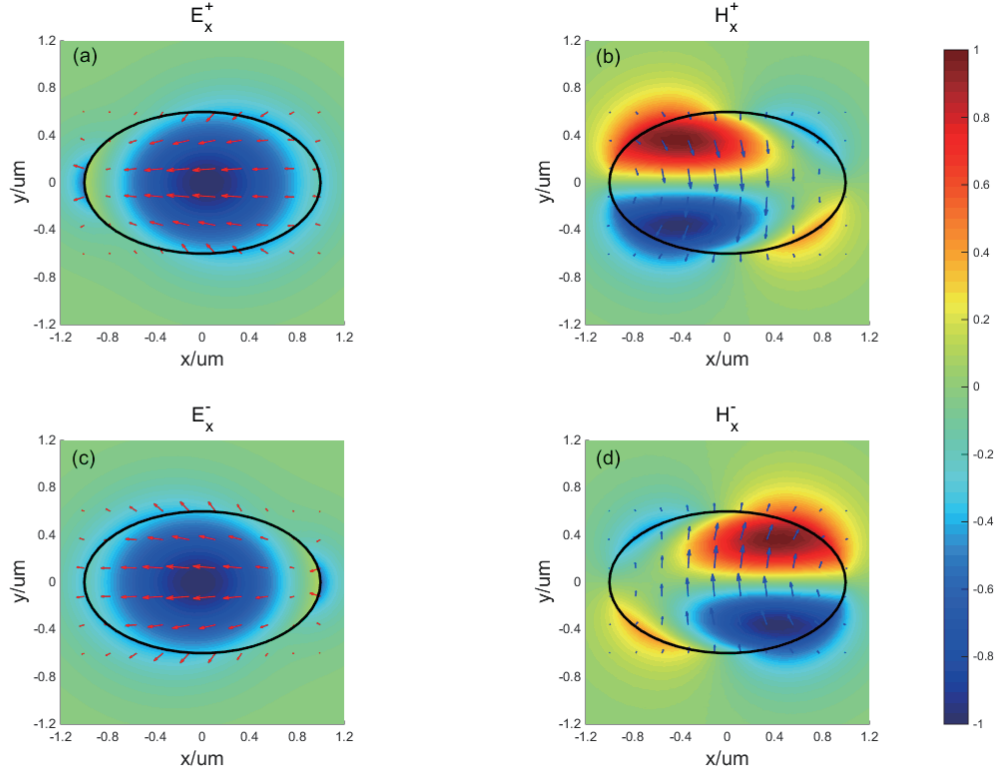


Fig. 2. The x -component as well as the vector field plots of the forward ((a)-(b)) and backward ((c)-(d)) propagating modes in anisotropic waveguide with ellipse-cross-section. The x -component of normalized electric/magnetic field is shown in (a,c)/(b,d), and the vector plots of the in-plane electric field (magnetic field) are also shown in (a,c)/(b,d) indicated by the arrows, the length of which is proportional to the magnitude of the vector field. In (a) and (c), the vector field plots take the real part of electric field, and the imaginary part of the magnetic field are taken in (b) and (d). Both the effective refractive index of forward and backward modes are 2.4668.

bifurcates. The exact bifurcation location of β in τ is coined as the exceptional point (EP). As evident in Fig. 1, the pair of modes with $n_{eff} = \beta/k_0$ of 1.61605 and 1.34651 ($\tau=0.4$) evolve to the modes with $n_{eff} = 1.44146 \pm 0.194268i$ ($\tau=1.2$) as τ crosses EP (in-between 0.4 and 1.2). As shown in Figs. 1 (a)-(d), the fields before EP remains unchanged under the subsequent \mathcal{P} ($\mathbf{r} \rightarrow -\mathbf{r}$) and \mathcal{T} (complex conjugation) operations. While both the eigen-fields and eigenvalues β of two modes after EP become conjugate complex to each other, see Figs. 1 (e)-(h), under the subsequent \mathcal{P} and \mathcal{T} operations. Hence, the symmetric relations of the eigen-fields and eigenvalues shown Fig. 1 is consistent with the predications by Eq. (11).

It is worthy to point out that the gain-loss balanced waveguide also obeys chiral symmetry, see discussion in Section 2.2. Provided one gets the eigen-field and eigenvalue β_0 of gain-loss balanced waveguides, as a consequence of chiral symmetry, $-\beta_0$ would also be the eigenvalue even after EP. And the relationship between the modes with opposite eigenvalue is just given by the chiral operation.

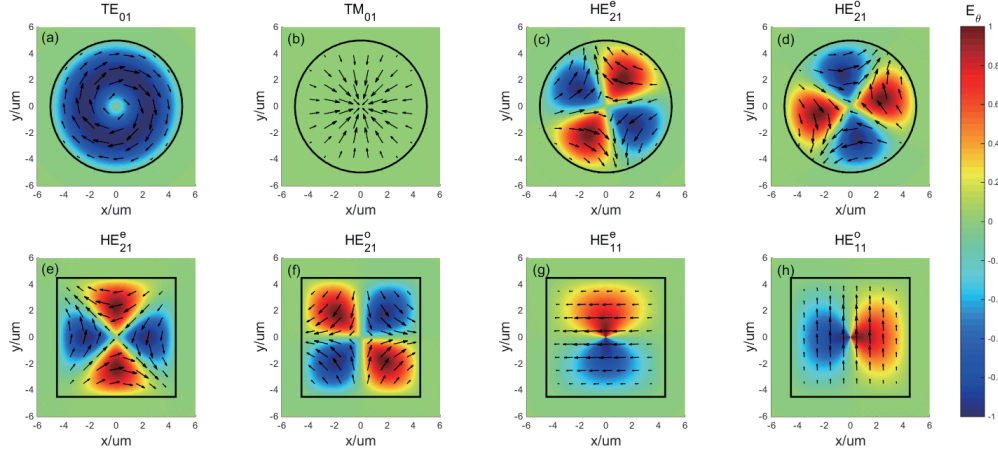


Fig. 3. (a-d) TE_{01} , TM_{01} , HE_{21}^e and HE_{21}^o in circular optical fibers. The four modes reduce into LP_{11} under weakly guiding. (e-h) HE_{21}^e , HE_{21}^o , HE_{11}^e and HE_{11}^o in square-core waveguide. The black circle or square indicate the borders of the waveguide-core, and arrows show the electric field orientation. The color plots are the azimuthal component, i.e., E_θ , of electric field. The radius of circle-core in (a-d) is $5 \mu m$, the relative permittivity ϵ_r is 4, and the background material is air. The effective refractive index is 1.99154 in (a), 1.99117 in (b), and 1.99135 in both (c) and (d). The length of square in (e-h) is $9 \mu m$, the material properties are the same as (a-d). The effective refractive index is 1.99118 in (e), 1.99093 in (f), and 1.99643 in both (g) and (h). Work wavelength is $1.55 \mu m$

3.2. Parity symmetry in anisotropic waveguides

To illustrate the parity symmetry, we consider an anisotropic waveguide as shown in Fig. 2. The cross-section of the waveguide is elliptical, thus has the C_{2z} symmetry, which is equivalent to the coordination transform $\mathbf{r} \rightarrow -\mathbf{r}$ in the 2D transverse plane. In the waveguide, the semi-major and semi-minor axis are $1 \mu m$ and $0.6 \mu m$, respectively. The relative permittivity

$$\text{is } \bar{\epsilon}_r = \begin{pmatrix} 10 & 0 & 4i \\ 0 & 10 & 0 \\ -4i & 0 & 10 \end{pmatrix} \text{ corresponding to magneto-optical materials, and the permeability } \mu_r$$

1, with background medium air. As predicated in Section 2.4, the transverse electric fields in backward propagating mode are same as that in forward mode under the parity operation ($\mathbf{r} \rightarrow -\mathbf{r}$), while the magnetic field transforms in a similar fashion but acquire an additional sign flip. Comparing Fig. 2 (a-b) with (c-d), it's clear that the electric field x component and magnetic field x component are consistent with the predications from Section 2.4.

3.3. Rotational symmetry in optical fiber

According to the dual symmetry of Maxwell equation, the two forward propagating modes Ψ_1 and Ψ_2 are degenerated provided $\epsilon_r = \mu_r$, which can be easily proved by exchanging the permittivity tensor and permeability tensor in the Hamiltonian. In the following, we will show that rotational symmetries in optical waveguides can protect the degeneracy of the two forward propagating modes Ψ_1 and Ψ_2 without $\epsilon_r = \mu_r$ via concrete examples, i.e., circular optical fiber or square optical waveguides, under certain conditions.

This differences between the pure TE/TM modes and the HE/EH modes lead to the following fact: one mode in each HE/EH mode pair within the aforementioned truncated mode set in circular fiber can be transformed to the other by rotating their transverse fields globally with a constant angle, such statement does not hold for pure TE/TM modes, see details in Appendix A.

As an example, we pick out four modes of optical fiber as shown in Fig. 3 (a-d). Two observations can be seen: (1) despite the variation of the rotational angle, the TE_{01} in Fig. 3 (a) or TM_{01} in Fig. 3 (b) can only be rotated to itself [14]; (2) while the field orientations of HE_{21}^e (Fig. 3(c)) and HE_{21}^o (Fig. 3(d)) can be exchanged by rotating $\pi/4$. In consistency with the discussion in Section 2.7, the operator $P_R(\theta) \Psi(R(\theta)^{-1} \mathbf{r})$ can be seen as a global rotation of the electric field orientation in Fig. 3 with angle θ . Therefore, the HE_{21}^e and HE_{21}^o satisfy Eq. (13) with the angle $\theta = \frac{\pi}{4}$. Moreover, for any HE/EH mode pair satisfies Eq. (13) with corresponding rotating angle, i.e., $\frac{\pi}{2}$ for HE_{11} ($l = 0$) and $\frac{\pi}{6}$ for HE_{31} ($l = 2$), the polarization degeneracy exists. Due to the fact that the circle-core fiber has continuous rotational symmetry, any HE/EH mode pair are degenerated. As for TE_{01} and TM_{01} , there is no such relation for any mode pair. As for a waveguide with discrete rotational symmetry, if the azimuthal quantum number (l) of modes are consistent with the discrete symmetry of waveguide core, the degeneracy emerges. Otherwise the degeneracy vanishes. For example, in square-core fiber, the HE_{21} shown in Figs. 3 (e)-(f) modes are not degenerate, because square is not invariant under rotating with $\frac{\pi}{4}$. However, the HE_{11} (Fig. 3(g-h)) modes in square-core fiber is also degenerate, since square cross section remains the same under rotation of $\frac{\pi}{2}$.

4. Conclusion

In conclusion, we provide a systematic approach to classify the symmetric properties of waveguide modes in presence of gain/losses, anisotropy/bi-anisotropy, as well as the rational symmetry in the geometric cross-section. By eliminating the longitudinal field components (e_z and h_z), we derive the waveguide Hamiltonian that fully characterizes the waveguide modes. With the proper symmetry operations, i.e., chiral/time reverse/ parity symmetry, associated with waveguide Hamiltonian, one can easily build up the relations between forward and backward propagating modes. As for the \mathcal{PT} symmetry, we can identity the symmetric properties of mode profile if the \mathcal{PT} symmetry is fulfilled. For the cross-section with rotational symmetry, we study how the rotation symmetry gives rise to the polarization degeneracy, illustrated by circular fiber and waveguide with square cross-section.

The derived Hamiltonian as well as the symmetry operation don't rely on any specific material parameters or chosen geometry, thus can be applied to any waveguide system, as long as certain symmetry relation (not limited within the symmetries discussed in the paper) is fulfilled. Importantly, our approach can be applied to analysis waveguide modes without knowing the exact field distribution, thus simplifies the modal analysis and can be useful for wave-guiding design.

Appendix A: Rotational symmetry of vector field in circular fiber

In circular fiber with strong guidance, the waveguide modes are described by TE_{0m} (transverse electric modes), TM_{0m} (transverse magnetic modes), and HE_{lm}^p and EH_{lm}^p (the last two are hybrid modes), depending on the existence and weighting of E_z and H_z . The indices l s represent the azimuthal quantum numbers, and m s radial quantum numbers. The pure TE and TM modes are special in the sense that all the field components have no azimuthal dependence in cylindrical coordinate (ρ, ϕ, z) , such as TE_{01} in Fig. 3 (a). We can reformulate Hamiltonian in polar coordinate,

$$H(\rho, \phi) = \begin{pmatrix} 0 & 0 & -\frac{\partial_\rho}{\rho} \frac{\partial_\phi}{k_0 \epsilon_r \rho} & \frac{\partial_\rho}{\rho} \frac{\partial_\rho}{k_0 \epsilon_r \rho} \rho + k_0 \mu_r \\ 0 & 0 & -\frac{\partial_\phi}{\rho} \frac{\partial_\phi}{k_0 \epsilon_r \rho} - k_0 \mu_r & \frac{\partial_\phi}{\rho} \frac{\partial_\rho}{k_0 \epsilon_r \rho} \rho \\ \frac{\partial_\rho}{\rho} \frac{\partial_\phi}{k_0 \mu_r \rho} & -\frac{\partial_\rho}{\rho} \frac{\partial_\rho}{k_0 \mu_r \rho} \rho - k_0 \epsilon_r & 0 & 0 \\ \frac{\partial_\phi}{\rho} \frac{\partial_\phi}{k_0 \mu_r \rho} + k_0 \epsilon_r & -\frac{\partial_\phi}{\rho} \frac{\partial_\rho}{k_0 \mu_r \rho} \rho & 0 & 0 \end{pmatrix}, \quad (18)$$

with eigenstate $\Psi = [e_\rho, e_\phi, h_\rho, h_\phi]^T$. For TE and TM modes, $\partial_\phi = 0$, thus $H(\rho, \phi)$ reduces to the form that only has anti-diagonal elements, leading to the decoupling of TE and TM modes with different eigenvalues. Thus, the TE and TM modes in circular fiber can never be degenerated, though they share the same quantum number (They are approximately degenerate with weak guidance).

Due the continuous rotational symmetry, all fields in optical fiber can be conveniently expressed as a ρ -function multiplied by a ϕ -function, where ρ and ϕ are the radial and azimuthal variables [15]. For a given TE/TM, or EH/HE mode labeled by the quantum number (m, l) , the transverse electric (magnetic) field can be written as

$$\mathbf{e}_t^{e/o} = J_m^1(\rho) \begin{pmatrix} \cos(l\phi) \\ \sin(l\phi) \end{pmatrix} \text{ or } \begin{pmatrix} \sin(l\phi) \\ -\cos(l\phi) \end{pmatrix}, \quad (19)$$

or

$$\mathbf{e}_t^{e/o} = J_m^2(\rho) \begin{pmatrix} \sin(l\phi) \\ \cos(l\phi) \end{pmatrix} \text{ or } \begin{pmatrix} -\cos(l\phi) \\ \sin(l\phi) \end{pmatrix}. \quad (20)$$

Evidently, in cylindrical coordinates, Eq. (19) represents $\text{EH}_{(l-1)m}$ modes when $l > 1$ or TE_{0m} and TM_{0m} modes when $l = 1$, while Eq. (20) for $\text{HE}_{(l+1)m}$ modes. If $l > 1$ and $(l-1)\theta = \frac{\pi}{2}$, we can have the field in Eq. (19) under the rotation by Eq. (13) given by

$$\begin{pmatrix} \cos(\theta) & -\sin(\theta) \\ \sin(\theta) & \cos(\theta) \end{pmatrix} \begin{pmatrix} \cos(l(\phi - \theta)) \\ \sin(l(\phi - \theta)) \end{pmatrix} = \begin{pmatrix} \cos(l\phi - (l-1)\theta) \\ \sin(l\phi - (l-1)\theta) \end{pmatrix} = \begin{pmatrix} \sin(l\phi) \\ -\cos(l\phi) \end{pmatrix}, \quad (21)$$

which means that for pair of EH modes, we can rotate one vector field with $\theta = \frac{\pi}{2(l-1)}$ to get another one. However, it's invalid for TE and TM modes due to $l = 1$. Similarly in Eq. (20), we have,

$$\begin{pmatrix} \cos(\theta) & -\sin(\theta) \\ \sin(\theta) & \cos(\theta) \end{pmatrix} \begin{pmatrix} \sin(l(\phi - \theta)) \\ \cos(l(\phi - \theta)) \end{pmatrix} = \begin{pmatrix} \sin(l\phi - (l+1)\theta) \\ \cos(l\phi - (l+1)\theta) \end{pmatrix} = \begin{pmatrix} -\cos(l\phi) \\ \sin(l\phi) \end{pmatrix}, \quad (22)$$

provided $(l+1)\theta = \frac{\pi}{2}$. This implies that for HE modes, we can rotate one vector field with $\theta = \frac{\pi}{2(l+1)}$ to get another one.

Acknowledgment

Y. Chen acknowledges financial support from the National Natural Science Foundation of China (Grant No. 61405067), and the Fundamental Research Funds for the Central Universities, HUST: 2017KFYXJJ027.